

Evolution of coronal mass ejections in the early stage

Xingming Bao ^{a,*}, Hongqi Zhang ^a, Jun Lin ^{b,c}, Yunchun Jiang ^b, Leping Li ^b

^a National Astronomical Observatories of China, Chinese Academy of Sciences, A20 Datun Road, Chaoyang District, Beijing 100012, China

^b Yunnan Astronomical Observatory, NAOC, CAS, P.O. Box 110, Kunming, Yunnan 650011, China

^c Harvard-Smithsonian Center for Astrophysics, 60 Garden Street, Cambridge, MA 02138, USA

Received 31 October 2006; received in revised form 24 January 2007; accepted 13 February 2007

Abstract

This work reports the investigation of two coronal mass ejections (CME) observed in white light, H α , EUV and X-ray by various instruments both in space and on ground on February 18, 2003 and January 19, 2005, respectively. The white light coronal images show that the first CME began with the rarefaction of a region above the solar limb and was followed by the formation of its leading edge at the boundary of the rarefying region at altitude of $0.46 R_{\odot}$ from the solar surface. The rarefaction coincided the slow rising phase of the filament eruption, and the CME leading edge was observed to form as the filament eruption started to accelerate apparently. In the early stage of the second CME, a bright loop was first observed above the solar limb with height of $0.37 R_{\odot}$ in EUV images. We found that the more gradual CMEs initial process, the larger the timing difference between CMEs and their associated flares. The lower part of the filament brightened in H α images as the filament rose to a certain height. These brightenings imply that the filament may be heated by magnetic reconnection below the filament in the early stage of the eruption. We suggest that the possible mechanism which led to the formation of the CME leading edge and cavity is magnetic reconnection which occurred under the filament when it reached a certain height.

© 2007 COSPAR. Published by Elsevier Ltd. All rights reserved.

Keywords: Coronal mass ejections; Flare; Filament eruption

1. Introduction

Coronal mass ejections (CMEs) are sudden expansions of magnetic field and plasma from the Sun toward interplanetary space. The early development of CMEs has been extensively studied for many years since it is closely related to the driving mechanisms of both eruptive prominence and solar flare. Zhang et al. (2001) showed that the initial phase of CMEs always occurred before the onset of their associated flares. Filament eruptions usually begin several minutes before impulsive phases of flares (Kahler et al., 1988). Since CME initiations are difficult to identify, filament eruptions are often observed before CMEs start. Therefore, initial filament activities are considered as a trigger for subsequent CMEs (Neupert et al., 2001). However,

the study of a slow CME by Srivastava et al. (2000) suggested that the CME and its associated prominence resulted from a common cause which is the global reconstruction of the coronal magnetic field. Harrison (1995) argued that CMEs and flares are the consequence of the same magnetic “disease” and one does not trigger the other.

Magnetic reconnection plays an important role in the above processes and in producing various morphological features (Martens and Kuin, 1989; Forbes and Priest, 1995; Lin and Forbes, 2000; Lin et al., 2004). With the system losing its mechanical equilibrium, the flux rope is thrust upward and the closed magnetic field is severely stretched such that it effectively opens up, and a current sheet forms in the wake of the flux rope separating two magnetic fields of opposite polarity. Through magnetic reconnection in the current sheet, the free energy stored in the magnetic field previously is converted into kinetic

* Corresponding author.

E-mail address: xbao@bao.ac.cn (X. Bao).

energy, which ejects the magnetic flux and plasma outward producing CMEs, and thermal energy, which heats the solar atmosphere producing solar flares with the separating flare ribbons on the solar surface and the growing flare loops in the corona as the most magnificent characteristics.

With the reconnected magnetic flux being sent towards the solar surface via the lower tip of the current sheet to produce the flare loop system, conservation of magnetic flux outside the diffusion region (or the current sheet) and the divergence-free of magnetic field everywhere require the same amount of the reconnected magnetic flux to be sent upward through the upper tip of the current sheet creating the fast expanding CME bubble. The plasma associated with the flux fills outer shell of the ejecta. Lin et al. (2004) and Lin and Soon (2004) tentatively identified the outer shell, the expanded bubble and the flux rope with the leading edge, void and core of the 3-component CME structure (Hundhausen et al., 1994; Low, 2001), respectively.

The trigger mechanism of CMEs has been an unsolved problem for a long time, which may relate to the gradual evolution of magnetic field in photosphere. Though we could not determine which mechanism directly causes CMEs, it is helpful for understanding the physical nature of CMEs to explore how various components of CMEs (such as leading edge and cavity) form and develop in the early stage. In this paper, we examined the exact temporal and spatial relationship between CME, filament eruption and flare after an eruption initiates.

2. Observation data

Most H α images used in this study were taken by PICS, which is a telescope with a removable occulting disk that allows us to observe the solar limb and the disk alternately. The field of view (FOV) of PICS ranges from 0 to $2.25 R_{\odot}$ and the cadence is 3 min. Conjoining the H α image of the disk and that of the limb makes it possible to capture the early stage of an eruptive prominence from the solar surface to the lower corona.¹ The EIT 195 Å images with cadence of 12 min allow us to study the evolution of the erupting filament in the lower corona and that the flare ribbons on the disk.

In this paper, we present the analysis of two CMEs that occurred from the solar northwest limb. The first one was associated with a polar crown filament eruption and a two-ribbon flare on February 18, 2003. The second one was associated with an X 1.3 flare on January 19, 2005. Though the X-ray flux of the flare in first eruption was weak, relatively slow initiation of this eruption allows us to examine the process in the early phase in detail. Unlike the first eruption, the second eruption shown an impulsive process in initial stage. The main purpose of this work is to

study the formation of various components of the CME and their temporal relation to the eruptive prominence as well as to the flare. Evolution in the morphological features of the two eruptions in the early stages observed at various wavelengths is also examined.

3. Results

3.1. A CME associated with a filament eruption

The early stage of the first eruption is displayed in Fig. 1 that includes the H α , the EIT 195 Å, and the soft X-ray images of the eruptive prominence. The upper rows of panels in Fig. 1 are the composite of the H α images of the disk and those with the solar disk blocked, so the clear structures of the filament both inside and outside the solar disk are visible (Fig. 1a through d). At 01:50 UT, the lower part of the filament became bright (indicated by the arrow in Fig. 1a) when the filament just lifted to about 9×10^4 km. At 01:59 UT the bright feature expanded to the other parts of the filament (indicated by the arrow in Fig. 1b) with the filament moving to 1.6×10^5 km. The prominence kept expanding at 02:11 UT (Fig. 1c), and its apex became invisible after 02:26 UT (Fig. 1d).

The EIT 195 Å and the soft X-ray counterparts of the above H α images are displayed in Fig. 1e through 1h and Fig. 1i through 1l, respectively. Comparing Fig. 1a and b with Fig. 1f and g, we noticed that brightening of the associated flare in H α occurred more early than that in EUV. With careful studying of the SXI movie, a fuzzy but visible filament profile is recognized as the filament lifted up, while the filament could hardly be discernable in X-ray images before it moved up (comparing Fig. 1a and i). The top of the filament in the SXI image (indicated by the arrow in Fig. 1j) appeared unusually bright relative to other part of the filament at 02:01 UT, and two bright points appeared in the footpoints of the filament. The bright point at the top of the filament disappeared immediately while the two bright points in the footpoints get brighter, corresponding to the H α and EIT 195 Å flare ribbons (Fig. 1k and l). This indicates that the top and the footpoints of the filament were heated to high temperature of more than 10^6 K. More compact bright points were also observed in the hard X-ray images (Aschwanden et al., 1996).

Before the eruptive prominence completely left the FOVs of PICS and EIT 195 Å images, the disturbance in the corona by the resultant CME could already be recognized in the MK4 white light images (Fig. 2), which show that the disturbance started with rarefaction of a region above the solar limb with area slightly increasing and the brightness decreasing gradually (Fig. 2a–c and accompanied gif animation²). The rarefaction was discernable from the environment around at 01:52 UT (indicated by the

¹ GIF animation is available at http://sun.bao.ac.cn/staff/baoxm/halpha_0218.gif

² http://sun.bao.ac.cn/staff/baoxm/mk4_0218.gif

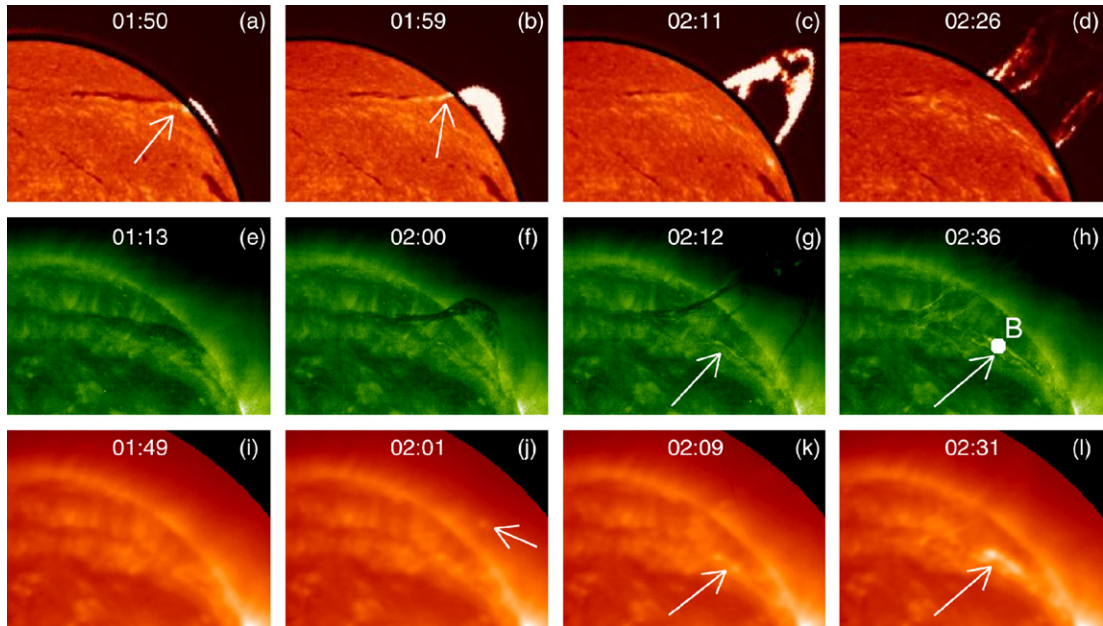


Fig. 1. Evolution of the 2003 February 18 event observed in various wavelengths. Top row of panels: composite of the PICS $H\alpha$ images of the limb and the disk. The white arrows indicate the emission features appeared in the lower part of the filament. Middle row of panels: EIT 195 \AA images, the white arrows indicate the flare ribbons. The bright region B in (h) indicates the area where the brightness of EIT 195 \AA images plotted in Fig. 2 was measured. Bottom row of panels: GOES Soft X-ray Imager (SXI) images, the white arrows indicate the brightenings in the top of the eruptive filament at 02:01 UT and flare ribbons at 02:09 UT and 02:31 UT respectively.

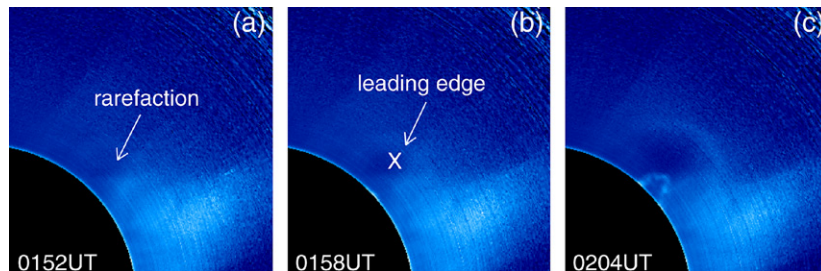


Fig. 2. Evolutions and formations of each component of the first CME that possessed the typical morphological features on February 18, 2003. (a) Rarefaction appeared above the solar limb. (b) Leading edge of the CME formed. The cross sign indicates the point where the brightness of the MK4 images was measured. (c) Prominence (core of CME), dark cavity and bright loop (CME leading edge) fully developed.

white arrow in Fig. 2a). At 01:58 UT the CME leading edge formed on the boundary of the rarefying region (Fig. 2b) at altitude of $1.46 R_{\odot}$ and became more significant as it reached to $1.65 R_{\odot}$ at 02:01 UT. The top of the filament just appeared over the limb of the occulting disk. The three-part structure of the CME (bright core, cavity and bright loop) fully formed at 02:04 UT as shown in Fig. 2c.

In order to show the time sequences of the filament eruption (initiation of the CME) and the associated flare, we plotted the height-time profiles of the filament and the CME leading edge as well as variations of the GOES X-ray flux in Fig. 3a, the brightness of the MK4 and EIT 195 \AA images in Fig. 3b, respectively. The brightness of the EIT 195 \AA image was measured from points within a circular area with the radius of five pixels located around the center of a flare ribbon (indicated by bright solid circle B in Fig. 1h), and we take the brightness of the flare as the maximum value of the brightness of this area. The bright-

ness of the MK4 image was measured at a fixed point located at a height about $1.3 R_{\odot}$ (indicated by the cross sign in Fig. 2b). Since the white light image results from the integral contribution of the Thomson-scattered photospheric radiation by electrons along the line of sight through the optically thin coronal plasma, the brightness in the MK4 white light images is proportional to the electron density in the corona. The variation of the brightness in coronal image is thus a quantitative indicator of change in the coronal material.

Comparing plots in Fig. 3a and b, we find that the soft X-ray flux began to increase gradually with the filament rising up after 01:58 UT, and the associated flare is of class B. Variation of the brightness of the MK4 coronal images, which indicated the initiation of the CME, could be divided into three stages. The first stage is the period when the brightness of the MK4 coronal images start to decrease gradually which indicates the rarefying process from

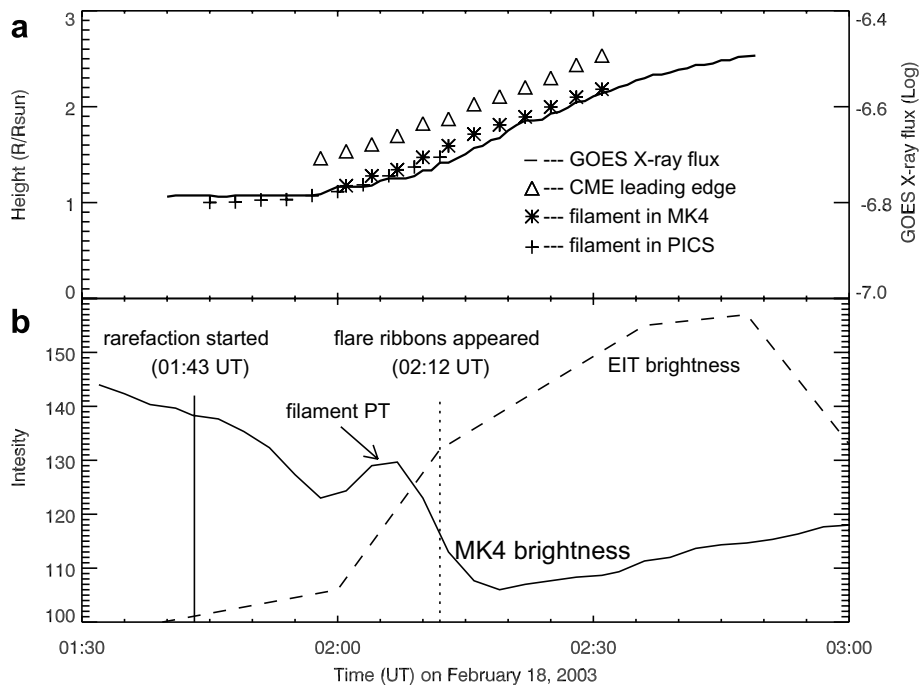


Fig. 3. Time sequences of the filament eruption, flare and CME. (a) The height-time profiles of the CME leading edge and the filament. The GOES X-ray flux is plotted in solid curve. (b) Variations of EIT 195 Å brightness (dashed curve) and of MK4 brightness (solid curve). The solid vertical line indicates the time when the rarefaction above the solar limb started and the dashed vertical line indicates the time when flare ribbons appeared in the EIT 195 Å images. The arrow filament PT indicates the increase of brightness during the period when the filament passed through the measuring point indicated by the cross sign in Fig. 2b.

01:43 UT (the solid vertical line in Fig. 3b) to 01:58 UT. Usually, the decrease of the brightness is difficult to discern from snapshots of the MK4 coronal images. We notice that the rarefying process is almost synchronized with the slow rising phase of the eruptive filament. In second stage (from 02:01 UT to 02:15 UT), the leading edge of the CME formed and brightness kept decreasing to the minimum. When the bright prominence in MK4 images passed through the measuring point (indicated by the cross sign in Fig. 2b), the brightness of MK4 images increased suddenly (indicated by the arrow filament PT in Fig. 3b) since the prominence is brighter than the dark cavity. In third stage the brightness began to increase gradually after 02:20 UT. The brightness of EIT 195 Å images which show the development of the flare ribbons began to increase obviously at 02:12 UT and reached the maximum at

02:48 UT. The flare ribbons appeared at 02:12 UT (indicated by the dashed vertical line in Fig. 2b) and the filament sped up at around 01:58 UT (Fig. 3a) after the CME front commenced to form.

3.2. A CME associated with an X1.3 flare

The second CME on 19 January 2005 is a halo CME with very fast average speed of 2000 km s^{-1} . The running difference images of the CME event are shown in Fig. 4. The X-ray flux started to rise apparently at 08:06 UT. A bright loop overlying several small loops appeared slightly over solar limb ($1.1 R_{\odot}$) at 08:00 UT. These loops merged into a larger loop at a height of $\sim 1.4 R_{\odot}$ at 08:10 UT. We are not sure if the large loop is the CME leading edge because no white light image in such a low height is

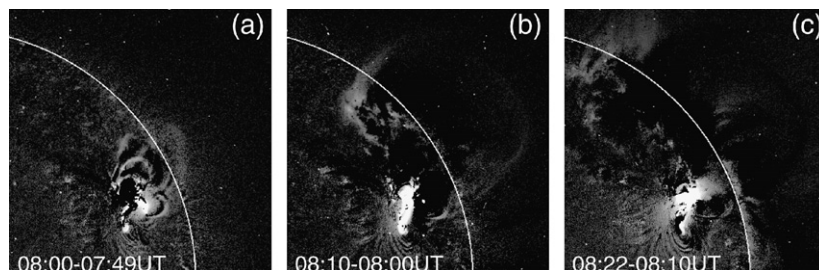


Fig. 4. EIT 195 Å running difference images of the second CME event on 19 January 2005. (a) A bright loop overlying several small loops appeared slightly over the solar limb at 08:00 UT. (b) The bright loop became visible at 08:10 UT. (c) Magnetic loops fully opened at 08:22 UT. White arch indicates the solar limb.

available. We notice that the flare ribbons and post-loops were not located in the center of the CME loop. At 08:22 UT, these CME loops fully opened. The CME leading edge first appeared in FOV of LASCO C2 at 08:29 UT with height of $3.7 R_{\odot}$. From the height-time profile, the bright loop in EIT 195 Å images could be identified as the leading edge of the CME in LASCO C2 white light images. Unfortunately, the CME occurred in the night of MLSO MK4, so no coronal image in the lower height range ($< 2 R_{\odot}$) was recorded.

4. Discussion and conclusions

Though the visible motion of the filament was identified in EIT 195 Å image between 00:00 UT and 00:12 UT, the slow rising of the filament started from 01:30 UT and rapid acceleration occurred from 02:00 UT. Meanwhile, we notice that the rarefying process of the first CME (indicated by the measurable decrease of MK4 brightness), which occurred during the period from 01:30 UT to 02:00 UT, is almost synchronized with slow rising of the filament. They were accelerated simultaneously. This indicates that both the CME and the eruptive filament were driven by the same mechanism (Srivastava et al., 2000).

From Fig. 3, we estimated that the onset of the first CME preceded its associated flare more than 30 min. The obvious timing difference between the CME and flare onset may closely relate to the gradual initiation of the first CME and filament eruption though the final speed of the CME is nearly 1000 km s^{-1} . From the EIT 195 Å difference images of the second CME in Fig. 4, shown that the CME may started around 08:00 UT, since the dimming structures appeared at 08:00 UT in Fig. 4a. GOES X-ray flux shown that the second flare onset occurred around 08:00 UT. So the onset of the CME and flare onset started within a time interval of 10 min.

Since the brightness in MK4 images is the indication of the plasma density, the rarefaction in the first eruption implies depletion of the plasma in the dark cavity above the solar limb in the lower corona, and the bright loop (CME leading edge) implies that the dense plasma was swept from the dark cavity to its boundary. The EIT 195 Å images reflect view of the low corona in $1.5 \times 10^6 \text{ K}$. In the case of on disk, the coronal dimming is due to mass-loss in the low corona (Harrison et al., 2003). The dense plasma in the low corona appears in dark absorption and the bright features represent active region. In the case of the second eruption of this work, the bright loops in Fig. 4b possibly correspond to the CME leading edge since the bright loop shows similar profile both in EUV and LASCO C1 images (Dere et al., 1997).

In addition to the first CME morphological features and their evolutions, another interesting phenomenon during the eruption is also worth mentioning. Some brightening features appearing in the lower part of the lifted section of the filament were observed in the stage of taking off. The first visible brightenings appeared at 01:50 UT when the

eruptive prominence reached about $9 \times 10^4 \text{ km}$ and then the bright features expanded to the two ends of the filament. Usually, the filament with dark structure appears as bright emission structure in dark background when it moved out of the solar disk. In the present case, however, the brightening features we observed are located in the inner part of the filament when it was still on the solar disk, instead of above the solar limb. Therefore, we rule out the possibility that brightening features in the lower part of the filament are due to its locating over the solar limb. Brightenings in our case should somehow result from heating of the cool filament material. Unlike the H α images, no EIT 195 Å emission was observed in filament when the filament reach to a certain height. The temperature of the filament in the EIT 195 Å image is more than $1.5 \times 10^6 \text{ K}$, this indicates that the temperature in the lower part of the filament ranges from 6×10^3 to 10^6 K . The bright point appeared on the top of the filament (indicated by the arrow in Fig. 1j) in SXI images, and lasted only few minutes. The bright features (flare ribbons) in the footpoints of the filament were observed in both H α , EIT 195 Å and SXI images.

Our main results in this study are summarized as following:

- (1) The leading edge of the first CME formed at height of $0.46 R_{\odot}$ as the rarefaction above the solar limb became obvious. This demonstrates that the CME initiated before its leading edge formed.
- (2) The initiation of the first CME which is shown by the rarefaction process in MK4 images is almost synchronized with the process of the slow rising. This indicates that the CME and the filament eruption started simultaneously.
- (3) The timing difference between CME and flare onset is closely related to the initial process of eruption. The more gradual the CME initiation, the larger the timing difference between CMEs and their associated flares.
- (4) The brightenings in H α images suggest that the filament may be heated by the magnetic reconnection occurred under it.

Acknowledgements

We would like to thank the MLSO, GOES and SOHO teams for supporting observation data. X.B. is grateful to J.L. and Y.J. for their hospitality when visiting to the Yunnan Astronomical Observatory. This work was supported by the National Natural Sciences Foundation of China (NSFC) under Grants 10233050, 10228307, 10611120338, 10373016 and 10473016 and the National Key Basic Research Program of China under Grants TG 2000078401 and 2006CB806301.

References

- Aschwanden, M.J., Hudson, H., Kosugi, T., Schwartz, R.A. *Astrophys. J.* 464, 985, 1996.

- Dere, K.P., Brueckner, B.E., Howard, R.A., et al. *Solar Phys.* 175, 601, 1997.
- Forbes, T.G., Priest, E.R. *Astrophys. J.* 446, 377, 1995.
- Harrison, R.A. *Astron. Astrophys.* 304, 585, 1995.
- Harrison, R.A., Bryans, P., Simnett, G.M., Lyons, M. *Astron. Astrophys.* 400, 1071, 2003.
- Hundhausen, A.J., Stanger, A.L., Serbicki, S.A., in: Hunt J.J., (ed.), *Solar Dynamic Phenomena and Solar Wind Consequences*, ESA-SP 373, Noordwijk: ESA, pp. 409, 1994.
- Kahler, S.W., Moore, R.L., Kane, S.R., et al. *Astrophys. J.* 328, 824, 1988.
- Lin, J., Forbes, T.G. *J. Geophys. Res.* 105 (A2), 2375, 2000.
- Lin, J., Raymond, J.C., van Ballegoijen, A.A. *Astrophys. J.* 602, 422, 2004.
- Lin, J., Soon, W. *New Astron.* 9, 611, 2004.
- Low, B.C. *J. Geophys. Res.* 106 (A11), 25141, 2001.
- Martens, P.C.H., Kuin, N.P.M. *Solar Phys.* 122, 263, 1989.
- Neupert, W.M., Thompson, B.J., Gurman, J.B., et al. *J. Geophys. Res.* 106 (A11), 25215, 2001.
- Srivastava, N., Schwenn, R., Inhester, B., et al. *Astrophys. J.* 534, 468, 2000.
- Zhang, J., Dere, K.P., Howard, R.A., et al. *Astrophys. J.* 559, 452, 2001.